PROCEEDINGS OF SPIE

SPIEDigitalLibrary.org/conference-proceedings-of-spie

An adaptive coherent flow power doppler beamforming scheme for improved sensitivity towards blood signal energy

Ozgun, Kathryn, Byram, Brett

Kathryn A. Ozgun, Brett C. Byram, "An adaptive coherent flow power doppler beamforming scheme for improved sensitivity towards blood signal energy," Proc. SPIE 10955, Medical Imaging 2019: Ultrasonic Imaging and Tomography, 109550H (15 March 2019); doi: 10.1117/12.2514184



Event: SPIE Medical Imaging, 2019, San Diego, California, United States

An adaptive coherent flow power Doppler beamforming scheme for improved sensitivity towards blood signal energy

Kathryn A. Ozgun and Brett C. Byram

Vanderbilt University, Nashville, TN, USA

ABSTRACT

Ultrasonic flow imaging remains susceptible to cluttered imaging environments, which often results in degraded image quality. Coherent Flow Power Doppler (CFPD)-a beamforming technique-has demonstrated efficacy in addressing sources of diffuse clutter. CFPD depicts the normalized spatial coherence of the backscattered echo, which is described by the van Cittert-Zernike theorem. However, the use of a normalized coherence metric in CFPD uncouples the image intensity from the magnitude of the underlying blood echo. As a result, CFPD is not a robust approach to study gradation in blood echo energy, which depicts the fractional moving blood volume. We have developed a modified beamforming scheme, termed power-preserving Coherent Flow Power Doppler (ppCFPD), which employs a measure of signal covariance across the aperture, rather than normalized coherence. As shown via Field II simulations, this approach retains the clutter suppression capability of CFPD, while preserving the underlying signal energy, similar to standard power Doppler (PD). Furthermore, we describe ongoing work, in which we have proposed a thresholding scheme derived from a statistical analysis of additive noise, to further improve perception of flow. Overall, this adaptive approach shows promise as an alternative technique to depict flow gradation in cluttered imaging environments.

Keywords: ultrasound, power Doppler, beamforming, coherence, blood flow

1. INTRODUCTION

Power Doppler (PD) ultrasound is a practical imaging technique used for the assessment of blood flow, offering a high frame rate and real-time capability. However, attaining adequate visualization of blood flow in all patients remains a clinical challenge. Extraneous 'clutter' signals imposed by thermal noise, off-axis scattering, and reverberation often degrade image quality and can result in incomplete radiologic examinations.¹

The need for improved clutter suppression has motivated the development of coherence-based beamformers. Spatial coherence is a measurement derived from statistical optics used to describe the similarity of a wavefront observed at two points in space. As described by the van Cittert-Zernike theorem, the spatial coherence of a wavefront emanating from an incoherent source is proportional to the Fourier transform of the transmit intensity profile. Mallart and Fink extended this theory to ultrasound, observing that echos produced by diffuse scattering media may be modelled as an incoherent source.² The predictable character of backscattered echos is leveraged by Coherent Flow Power Doppler imaging, which uses spatial coherence as the basis of image formation rather than the magnitude of echo reflectivity. In a number of studies, Coherent Flow Power Doppler has demonstrated greater sensitivity toward blood flow in cluttered environments, in comparison to conventional power Doppler.^{3,4}

However, a drawback of Coherent Flow Power Doppler (CFPD) beamforming is that image intensity is disassociated from the received echo magnitude. Observing the blood echo power is clinically valuable, as it is indicative of the concentration of blood scatterers. Power Doppler image intensity is linearly proportional to this quantity, also referred to as the fractional moving blood volume.⁵ Since CFPD beamforming employs a measure of normalized spatial coherence, CFPD image intensity exhibits a non-linear response toward echo magnitude and is affected by the relative signal-to-noise ratio.⁶ As a result, CFPD image intensity is not a robust indicator of flow gradation.

Further author information: (Send correspondence to K.A.O.)

K.A.O.: E-mail: kathryn.a.ozgun@vanderbilt.edu, Telephone: (443) 974-8026

B.C.B.: E-mail: brett.c.byram@vanderbilt.edu, Telephone: (615) 343-2327

Medical Imaging 2019: Ultrasonic Imaging and Tomography, edited by Brett C. Byram, Nicole V. Ruiter, Proc. of SPIE Vol. 10955, 109550H ⋅ © 2019 SPIE CCC code: 1605-7422/19/\$18 ⋅ doi: 10.1117/12.2514184

Herein, we describe a coherence-based beamforming technique termed power-preserving Coherent Flow Power Doppler (ppCFPD), which adapts CFPD to preserve encoding of the blood echo magnitude in the image intensity. The objective of this work is to demonstrate that the ppCFPD technique preserves the blood echo magnitude, while maintaining superior rejection of incoherent clutter signals in comparison to conventional power Doppler. We additionally introduce a statistical expression describing the effect of additive noise on image intensity, which may be used to threshold the image and further improve sensitivity toward blood flow in cluttered environments.

2. IMAGE FORMATION TECHNIQUES

2.1 Power Doppler

Power Doppler is a conventional technique for blood flow imaging, which depicts the integrated echo amplitude. In PD image formation, beamformed RF-data is filtered to suppress temporally stationary clutter. The filtered RF-data is then integrated over a temporal ensemble of length A, as

$$PD = \sum_{a=1}^{A} |RF(a)|^{2}.$$
 (1)

A two-dimensional autocorrelation approach has also been introduced, which reduces random fluctuations by averaging over an axial kernel, as described by Loupas et. al. 8

2.2 Coherent Flow Power Doppler

The CFPD image formation technique developed by Dahl et. al depicts the normalized spatial coherence of the backscattered echo. Received echos are time-delayed and filtered to suppress stationary clutter. The normalized spatial coherence is then computed between pairs of delayed, filtered channel signals as a function of the spatial separation, or 'lag'.

The normalized spatial coherence, R(m), for an aperture of size N may be written

$$R(m) = \frac{1}{N-m} \sum_{i=1}^{N-m} \frac{\sum_{n=n_1}^{n_2} y_i(n) y_{i+m}(n)}{\sqrt{\sum_{n=n_1}^{n_2} y_i^2(n) \sum_{n=n_1}^{n_2} y_{i+m}^2(n)}},$$
 (2)

which is calculated for all pairs of time-delayed, filtered channel signals, y_i and y_{i+m} , separated by a given lag, m. To reduce random errors, fast-time averaging over a kernel, n, spanning approximately one wavelength is employed.

Measurement of the normalized spatial coherence is then repeated for a set of M successive lags, and averaged to produce the Short Lag Spatial Coherence metric, 9 which is

$$V(a) = \frac{1}{M} \sum_{m=1}^{M} R(m).$$
 (3)

The CFPD image is then reconstructed through integration of the squared SLSC metric,

$$CFPD = \sum_{a=1}^{A} V(a)^2. \tag{4}$$

For clarity, the term 'normalized spatial coherence' used herein will refer to the metric used in CFPD beamforming, as shown in Equation (2); the term 'spatial coherence' will refer to the metric used in ppCFPD beamforming, as written in Equation (5).

2.3 Power Preserving Coherent Flow Power Doppler

The proposed ppCFPD image formation technique depicts the spatial coherence, or mutual intensity, of the backscattered echo. The mutual intensity can be more difficult to interpret in comparison to normalized coherence, as the resultant value is scaled by the relative covariance of the signal intensities. However, the spatial coherence of signals measured across the aperture can be theoretically described through an assessment of the van Cittert-Zernike theorem.^{2,7}

As performed in CFPD, received echos are time-delayed and filtered to suppress stationary clutter. Omission of the denominator in Equation (2) yields the spatial coherence. For a given lag, m, the spatial coherence for an aperture of size N is

$$\check{R}(m) = \frac{1}{N-m} \sum_{i=1}^{N-m} \sum_{n=n_1}^{n_2} y_i(n) y_{i+m}(n),$$
(5)

which is calculated for all pairs of time-delayed channel signals, y_i and y_{i+m} . To reduce random errors, fast-time averaging over a kernel described by n, spanning approximately one wavelength is employed.

Subsequent averaging of the spatial coherence for an ensemble of M successive lags yields

$$\check{V}(a) = \frac{1}{M} \sum_{m=1}^{M} \check{R}(m).$$
(6)

The ppCFPD image is then reconstructed via summation over a temporal ensemble of size A, shown below in Equation (7). The use of spatial coherence, and omitting the squaring term used in Equation (4), effectively yields units of amplitude squared. As a result, the amplitude of blood signals in a ppCFPD image exhibits a dynamic range similar to power Doppler.

$$ppCFPD = \sum_{a=1}^{A} \check{V}(a) \tag{7}$$

2.4 The Effect of Noise on ppCFPD Image Intensity

The effect of noise power on the normalized spatial coherence metric has been previously described by Bottenus et al.^{6,10} An extension of this derivation has been performed to describe the effect of additive noise on the spatial coherence metric used in Equation (5).⁷ From this derivation, we note that the spatial coherence theoretically yields an estimate of the blood echo power that is independent of additive noise, excluding the zero-lag value. As supported in prior research, the spatial coherence of an incoherent noise signal is well-modelled by a delta function at lag zero.¹¹

However, in application, a small amount of uncorrelated noise may persist at non-zero lags due to random partial correlations. This residual noise signal is often low amplitude, but may misguide visual assessment. In addition, negative pixels may be produced in ppCFPD image formation. These values arise due to partial and out-of-phase correlations, which are associated with noise. Negative pixels are detrimental to image quality and inhibit log compression; thus, we have previously set negative pixels to zero when displaying images and calculating image quality metrics, which is consistent with prior literature. 12, 13

To robustly suppress residual additive noise, and justify the elimination of negative pixel values, we propose the use of a statistically-driven threshold. Additive noise may be modelled as a statistically independent process from the blood signal, thus we may develop a probabilistic model of noise signal intensity in ppCFPD images by considering a case in which channel data only contains noise.

2.4.1 Expression of ppCFPD Pixel Intensity

Assume that the channel data only contains noise, which we may model as an independent, normally distributed random variable with constant variance, distributed identically across all elements. It can be noted that the spatial coherence shown in (2) may be expressed in terms of the normalized correlation coefficient, $\rho(m)$, measured between signals y_i and y_{i+m} . Asserting the assumption of constant variance, we may pose an expression for the ppCFPD pixel intensity for channel data containing only noise as

$$ppCFPD = AH\sigma_{noise}^2 \frac{1}{M} \sum_{m=1}^{M} \frac{1}{N-m} \sum_{i=1}^{N-m} \rho(m).$$
 (8)

2.4.2 Statistical Assessment of Pixel Intensity

Small-valued correlation coefficients, as expected to be measured between two uncorrelated noise signals, are approximately equal to their respective z-score. For modelling simplicity, we approximate the probability distribution of the correlation coefficient with the distribution of the z-score. The z-score, obtained via the Fisher transform, is normally-distributed with a calculable mean and standard deviation. Using properties of location-scale probability distributions, we can generalize this to model the probability distribution of ppCFPD pixel intensity; thus, we find that the pixel intensity is approximately normally distributed with zero-mean and a variance of

$$\sigma_{pixel}^2 = A(\frac{1}{M}H\sigma_{noise}^2\sigma_z)^2 \sum_{m=1}^M \frac{1}{N-m}.$$
 (9)

The derivations of Equations (8) and (9) are omitted here for brevity, but will be given elsewhere. In application, the noise variance may be expressed in terms of the signal-to-noise ratio, which can be estimated via a lag-one autocorrelation.¹⁴

2.4.3 Definition of a Confidence Interval

Using the statistical model of ppCFPD pixel intensity for noise signals, we can define a threshold as the upper bound of the 95% statistical confidence interval of expected intensity. For a given pixel, x, this may be written

$$f(x) = \begin{cases} x, & \text{if } x \ge 1.96 \ \sigma_{pixel} \\ 0, & \text{otherwise} \end{cases}$$
 (10)

3. METHODS

3.1 Simulated Flow Phantoms

For this investigation, simulated flow data was obtained using coherently compounded, steered plane waves. Simulated data was generated using Field II to study the performance of ppCFPD under varied conditions of clutter. The simulated phantom included a single blood vessel with a 5mm diameter, embedded in a 9cm-by-5cm homogeneous tissue block at a 45° angle relative to the transducer. Laminar blood flow was simulated using scatterers moving in a parabolic flow pattern, with a maximum velocity of 5cm/sec. The simulated acquisitions were performed using a 128-element linear transducer with a center frequency of 3MHz and pitch of 0.257mm. For each acquisition, plane waves between -4° and 4° spaced by 1° were simulated at a PRF of 9KHz. The channel data were delayed using Plane Wave Synthetic Focusing (PWSF) as described by Montaldo et al., in which the delayed channel data acquired at consecutive angles were summed to produce a final PRF of 1KHz. The A 2Hz IIR filter cutoff was used for temporal clutter suppression for the fractional moving blood volume assessment, and a 10Hz IIR filter was used to assess the validity of the theoretical threshold.

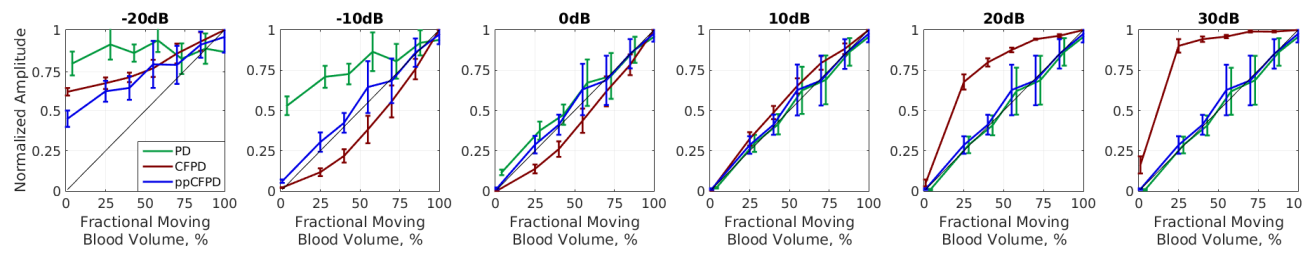


Figure 1. The ppCFPD blood signal amplitude remains a linear approximation of the fractional moving blood volume despite variation in the blood signal-to-noise ratio from -20dB to 30dB. This may be observed in the figure, as the ppCFPD curve closely approximates the theoretical value, shown in black.

3.2 Preservation of Blood Echo Magnitude

Preservation of blood signal energy was evaluated in terms of the capacity to resolve the fractional moving blood volume, in accordance with a prior power Doppler assessment by Rubin et al.⁵ The intensity of a power Doppler signal encodes the fraction of moving blood scatterers incurring a Doppler shift, which indicates relative vascularity. This was assessed by incrementally decreasing the fraction of moving blood scatterers, until nearly all blood scatterers remained stationary. Five independent simulations of blood and tissue were generated for each fractional step. Additionally, discrimination of fractional moving blood velocity was studied in the presence of added noise at six blood signal-to-noise levels.

3.3 Theoretical Threshold

Algorithm validation was performed by assessing the efficacy of the theoretical bound under two conditions: first, for a case in which the delayed channel signals contained only additive white noise, which aligned with the assumptions of the derivation; secondly, validation was performed for a dataset simulated in Field II containing noise, blood, and tissue, as described in Section 3.1. In simulation, the theoretical bound was compared to the 'true' empirically-measured 95% confidence interval, where a region-of-interest containing only noise was used to estimate the noise variance.

3.4 Image Quality Assessment

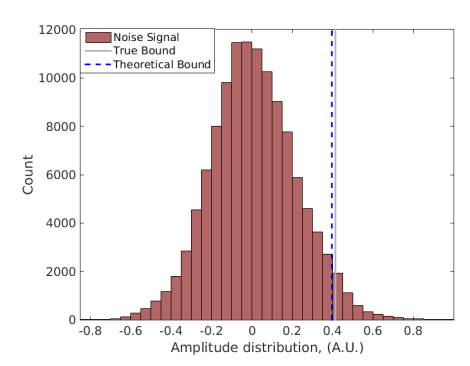
In order to evaluate the performance of the ppCFPD algorithm, we assessed image quality and perfusion characteristics. Results were compared with PD and CFPD images generated from the same datasets. The image quality metrics included contrast, contrast-to-noise (CNR), and root-mean-square signal-to-noise (SNRrms) calculations, as described in prior work.⁷

4. RESULTS AND DISCUSSION

Assessment of ppCFPD simulation results yielded up to a 13.9dB improvement in root-mean-square SNR, a 15.5dB gain in contrast, and an increase of 1.4 in CNR in comparison to PD images. In addition, blood pixel intensity remained linearly proportional to the fractional moving blood volume, as shown in Figure 1. In comparison, we observed that the CFPD image intensity remained sensitive to variations in noise power, which is supported by work completed by Bottenus and Trahey.⁶

Preliminary evaluation of the statistical thresholding scheme demonstrated feasibility. The correlation measured between simulated noise signals appears to be effectively modelled as a Gaussian process. Furthermore, extension of this model to ppCFPD pixel intensity appears to remain valid in simulation, as depicted in Figure 2. The theoretical threshold remained an effective approximation of the empirically-measured bound for single-vessel simulations, which additionally affirms the assumption that the noise is a statistically independent process from blood signals.

This preliminary work also justifies the thresholding of negative pixel values, as used in image quality metrics and prior studies. As shown in Figure 2a, the distribution of noise pixel intensity is a zero-mean process. In comparison, blood signals were observed to have positive pixel distributions. However, the application of an adaptive threshold more robustly suppresses additive noise, as shown in Figure 3. Our future studies will seek to optimize the theoretical thresholding scheme to improve visualization of blood flow in cluttered environments.



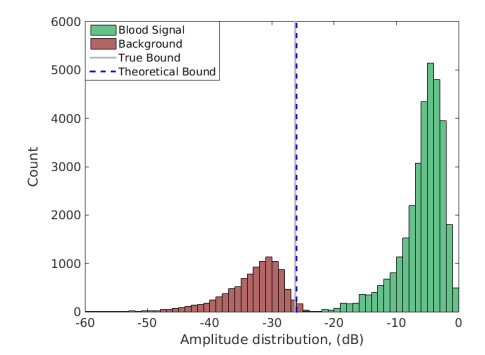


Figure 2. (a) Distribution of pixel intensity for channel data containing only noise. The theoretical threshold is an effective approximation of the 95% confidence interval, compared to the empirically measured value. (b) The confidence interval remained a robust approximation of noise pixel variance for simulations additionally containing blood.

5. CONCLUSIONS

We have theoretically described the anticipated nature of the ppCFPD beamforming technique, and its efficacy has been demonstrated through a preliminary investigation. The ppCFPD beamforming scheme mitigates diffuse clutter through the application of an aperture domain coherence measure, which improves the perception of vasculature in cluttered environments. The resultant image intensity portrays an approximation of the underlying blood signal energy, which addresses the primary drawback of employing a normalized coherence measure in conventional CFPD. Furthermore, the ppCFPD beamforming technique is robust to additive noise, which restricts the efficacy of conventional power Doppler. Overall, this approach shows promise for improving discrimination of blood flow within cluttered environments. Both CFPD and ppCFPD offer improved image quality over PD; however, we demonstrated that the CFPD technique exhibited non-linear characteristics as a function of varied SNR. In comparison, ppCFPD was robust to thermal noise power and retained sensitivity to variation in fractional moving blood volume. This preliminary study suggests that the use of ppCFPD in conjunction with a theoretical threshold may be a valuable approach to assess blood flow gradation in cluttered imaging environments.

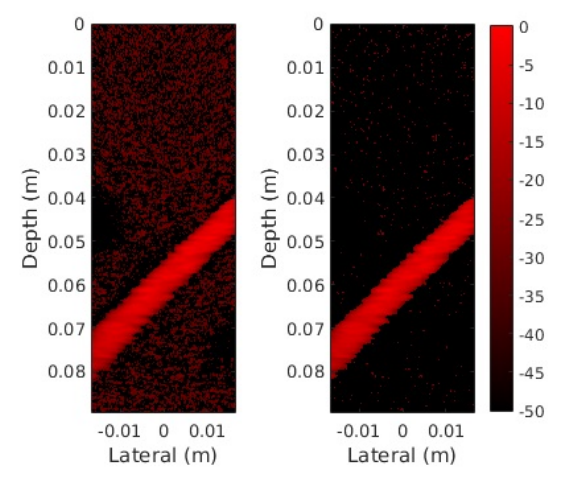


Figure 3. Depiction of ppCFPD image with thresholding of negative pixels (left) and with the theoretical threshold (right). Perception of blood flow is improved when the theoretical threshold is applied, as pixels containing noise are more effectively suppressed.

ACKNOWLEDGMENTS

The authors would like to thank the staff of the Vanderbilt University ACCRE computing resource. This work was supported by NIH-NIBIB award T32-EB021937 and NSF award IIS-1750994.

REFERENCES

- [1] Dahl, J., Hyun, D., Li, Y., Jakovljevic, M., Bell, M. A. L., Long, W. J., Bottenus, N., Kakkad, V., and Trahey, G. E., "Coherence beamforming and its applications to the difficult-to-image patient," *IEEE International Ultrasonics Symposium*, 1–10 (2017).
- [2] Mallart, R. and Fink, M., "The van cittert-zernike theorem in pulse echo measurements," *The Journal of the Acoustical Society of America* **96** (1991).
- [3] Li, Y. and Dahl, J., "Coherent flow power doppler (cfpd): Flow detection using spatial coherence beamforming," *IEEE Transactions on Ultrasonics, Ferroelectrics, and Frequency Control* **62**, 1022–1035 (2015).
- [4] Li, Y. L., Hyun, D., Abou-Elkacem, L., Willmann, J. K., and Dahl, J. J., "Visualization of small-diameter vessels by reduction of incoherent reverberation with coherent flow power doppler," *IEEE transactions on ultrasonics, ferroelectrics, and frequency control* **63**(11), 1878–1889 (2016).
- [5] Rubin, J. M., Adler, R. S., Fowikes, J. B., Spratt, S., Pallister, J. E., Chen, J.-F., and Carson, P. L., "Fractional moving blood volume: estimation with power doppler us,," RSNA Radiology 197 (1995).
- [6] Bottenus, N. B. and Trahey, G. E., "Equivalence of time and aperture domain additive noise in ultrasound coherence," *Journal of the Acoustical Society of America* 137 (2015).
- [7] Ozgun, K. A., Tierney, J. E., and Byram, B. C., "An adapted coherent flow power doppler beamforming scheme for improved sensitivity towards blood signal energy," 2018 IEEE International Ultrasonics Symposium (IUS) (2018).
- [8] Loupas, T., Peterson, R., and Gill, R. W., "Experimental evaluation of velocity and power estimation for ultrasound blood flow imaging, by means of a two-dimensional autocorrelation approach," *IEEE transactions on ultrasonics, ferroelectrics, and frequency control* **42**(4), 689–699 (1995).
- [9] Lediju, M. A., Trahey, G. E., Byram, B. C., and Dahl, J. J., "Short-lag spatial coherence of backscattered echoes: Imaging characteristics," *IEEE transactions on ultrasonics, ferroelectrics, and frequency control* 58(7) (2011).
- [10] Bottenus, N., "Recovery of the complete data set from focused transmit beams," *IEEE transactions on ultrasonics, ferroelectrics, and frequency control* **65**(1), 30–38 (2018).
- [11] Pinton, G., Trahey, G., and Dahl, J., "Characteristics of the spatial coherence function from backscattered ultrasound with phase aberration and reverberation clutter," in [Ultrasonics Symposium (IUS), 2011 IEEE International], 684–687, IEEE (2011).
- [12] Nair, A. A. and Bell, M. A. L., "Robust short-lag spatial coherence imaging," *IEEE Transactions on Ultrasonics, Ferroelectrics, and Frequency Control* **65**, 366–377 (2018).
- [13] Stanziola, A., Leow, C. H., Bazigou, E., Weinberg, P. D., and Tang, M.-X., "Asap: Super-contrast vasculature imaging using coherence analysis and high frame-rate contrast enhanced ultrasound," *IEEE transactions on medical imaging* 37(8), 1847–1856 (2018).
- [14] Long, W., Bottenus, N., and Trahey, G. E., "Lag-one coherence as a metric for ultrasonic image quality," *IEEE transactions on ultrasonics, ferroelectrics, and frequency control* **65**(10), 1768–1780 (2018).
- [15] Jensen, J. A., "Field: A program for simulating ultrasound systems," in [10th Nordicbaltic conference on biomedical imaging], 4, Citeseer (1996).
- [16] Jensen, J. A. and Svendsen, N. B., "Calculation of pressure fields from arbitrarily shaped, apodized, and excited ultrasound transducers," *IEEE transactions on ultrasonics, ferroelectrics, and frequency control* **39**(2), 262–267 (1992).
- [17] Montaldo, G., Tanter, M., Bercoff, J., Benech, N., and Fink, M., "Coherent plane-wave compounding for very high frame rate ultrasonography and transient elastography," *IEEE Transactions on Ultrasonics, Ferroelectrics, and Frequency Control* **56**, 489–506 (2009).